

## Low-density approach to the Kondo-lattice model

W. Nolting,<sup>1</sup> G. G. Reddy,<sup>2</sup> A. Ramakanth,<sup>2</sup> and D. Meyer<sup>3</sup>

<sup>1</sup>Humboldt-Universität zu Berlin, Institut für Physik, Lehrstuhl Festkörpertheorie, Invalidenstrasse 110, 10115 Berlin, Germany

<sup>2</sup>Kakatiya University, Department of Physics, Warangal-506009, India

<sup>3</sup>Department of Mathematics, Imperial College, 180 Queen's Gate, London SW7 2BZ, United Kingdom

(Received 23 May 2001; published 25 September 2001)

We propose an approach to the (ferromagnetic) Kondo-lattice model in the low-density region, where the model is thought to give a reasonable framework for manganites with perovskite structure exhibiting the colossal magnetoresistance effect. Results for the temperature-dependent quasiparticle density of states are presented. Typical features can be interpreted in terms of elementary spin-exchange processes between itinerant conduction electrons and localized moments. The approach is exact in the zero-bandwidth limit for all temperatures and at  $T=0$  for arbitrary bandwidths, fulfills exact high-energy expansions, and reproduces correctly second-order perturbation theory in the exchange coupling.

DOI: 10.1103/PhysRevB.64.155109

PACS number(s): 71.10.Fd, 75.30.Mb, 75.30.Vn

### I. INTRODUCTION

The Kondo-lattice model<sup>1</sup> (KLM) describes the interplay of itinerant electrons in a partially filled energy band with quantum mechanical spins (magnetic moments) localized at certain lattice sites. Characteristic model properties result from an interband exchange interaction between the two subsystems.

On the one hand, the energy band structure is modified by the magnetic state of the spin system (temperature dependences, band splittings, band deformations), while, on the other, the magnetic state of the spin system is affected by the itinerant electrons because the KLM does not incorporate a direct exchange between the moments. The model Hamiltonian consists of two parts

$$H = H_s + H_{sf}. \quad (1)$$

$H_s$  is the kinetic energy of itinerant band electrons,

$$H_s = \sum_{ij\sigma} T_{ij} c_{i\sigma}^\dagger c_{j\sigma}, \quad (2)$$

where  $c_{i\sigma}^\dagger$  ( $c_{i\sigma}$ ) is the creation (annihilation) operator of a band electron specified by the lower indices.  $T_{ij}$  are the hopping integrals. The second term in Eq. (1) is an interband exchange term with coupling strength  $J$ , written as an intra-atomic interaction between the conduction electron spin  $\sigma_i$  and the localized magnetic moment represented by the spin operator  $\mathbf{S}_i$ :

$$H_{sf} = -J \sum_i \sigma_i \cdot \mathbf{S}_i. \quad (3)$$

According to the sign of the exchange coupling  $J$ , a parallel ( $J>0$ ) or an antiparallel ( $J<0$ ) alignment of itinerant and localized spins is favored with remarkable differences in the physical properties. The parallel ( $J>0$ ) orientation is often referred to as the ferromagnetic Kondo-lattice model (FKLM), alternatively known as the  $s$ - $f$  or  $s$ - $d$  model. The applications of the KLM are manifold.

### A. Magnetic semiconductors

Prototypes are the europium chalcogenides  $\text{EuX}$  ( $X = \text{O, S, Se, Te}$ ),<sup>2</sup> which are known to exhibit a spectacular temperature dependence of the band states. The redshift of the optical absorption edge upon cooling<sup>2,3</sup> from  $T=T_c$  to  $T=0$  K is due to a corresponding shift of the lower conduction band edge. There is clear evidence that in these materials the exchange  $J$  is positive, typically of order some tenths of eV. The coupling can therefore be classified as weak to intermediate.

### B. Semimagnetic semiconductors

In systems like  $\text{Cd}_{1-x}\text{Mn}_x\text{Te}$  and  $\text{Hg}_{1-x}\text{Fe}_x\text{Se}$  randomly distributed  $\text{Mn}^{2+}$  or  $\text{Fe}^{2+}$  ions provide localized magnetic moments which influence, via the exchange mechanism  $J$ , the band states of the II-VI semiconductors  $\text{CdTe}$  and  $\text{HgSe}$ . For moderate doping  $x$ , the moments do not order collectively so that a striking temperature dependence, such as that of the magnetic semiconductors ( $\text{EuX}$ ), cannot be expected. However, an anomalous magnetic field dependence of optical transitions and therewith of the band structure is observed<sup>4</sup> ("giant Zeeman splitting"). From the appropriate experimental data,  $J>0$  can be concluded. The coupling must be classified as weak.

### C. Local-moment metals

In ferromagnetic metals such as the rare earth element Gd, the magnetism is due to strictly localized  $4f$  electrons while the conductivity properties are determined by itinerant ( $5d, 6s$ ) electrons. The  $T=0$  moment of Gd is found to be  $7.63\mu_B$ .<sup>5</sup>  $7\mu_B$  stem from the exactly half-filled  $4f$  shell. The excess moment of  $0.63\mu_B$  originates from an induced spin polarization of the *a priori* nonmagnetic conduction bands, indicating a weak or intermediate coupling  $J>0$ .<sup>6</sup> Many of the recent research activities have been focused on the temperature dependence of the induced exchange splitting. Is it collapsing for  $T \rightarrow T_c$  or does it persist even in the paramagnetic phase?<sup>6,7</sup> The  $J$ -induced correlation and quasiparticle effects in the valence and conduction bands of Gd (or

equivalently Dy or Tb) lead to highly complex and therefore controversial photoemission data,<sup>8,9</sup> the interpretation of which is far from settled (see the review in Ref. 7). While the magnetic ordering of the semiconductors and insulators (class A) has to be explained via special superexchange mechanisms, which is beyond the field of application of the FKLM, it is commonly accepted that the collective magnetism of the local-moment metals is caused by the Ruderman-Kittel-Kasuya-Yosida (RKKY) interaction. The latter is also based on the exchange interaction  $J$ . The FKLM therefore provides, at least in a qualitative manner, a self-consistent description of magnetic and electronic properties of materials such as Gd.<sup>6,10</sup>

#### D. Manganite perovskites

Since the discovery of the colossal magnetoresistance (CMR),<sup>11,12</sup> the manganese oxides with perovskite structures  $T_{1-x}D_x\text{MnO}_3$  ( $T = \text{La, Pr, Nd}$ ;  $D = \text{Sr, Ca, Ba, Pb}$ ) have attracted great scientific interest. The prototypes  $\text{La}_{1-x}(\text{Ca, Sr})_x\text{MnO}_3$  have long been known for the “double exchange” mechanism.<sup>13</sup> Replacing in  $\text{La}^{3+}\text{Mn}^{3+}\text{O}_3$  a trivalent  $\text{La}^{3+}$  ion by a divalent alkali-earth ion ( $\text{Ca}^{2+}, \text{Sr}^{2+}$ ) requires an additional electron from the manganese for the binding. The result is a homogeneous valence mixture of the manganese ion ( $\text{Mn}_{1-x}^{3+}\text{Mn}_x^{4+}$ ). The three  $3d-t_{2g}$  electrons of  $\text{Mn}^{4+}$  are considered as more or less localized, forming a local  $S=3/2$  spin. The fourth electron in  $\text{Mn}^{3+}$  is of  $3d-e_g$  type and is itinerant. It is assumed that it interacts via intrashell Hund’s rule coupling (double exchange model<sup>14</sup>) with the  $S=3/2$  spins. The manganites are bad electrical conductors. It has therefore to be assumed that the intraatomic coupling  $J>0$  is much stronger than the hopping matrix element  $|t|$  ( $J \gg |t|$ ). Theoretical estimates for the bandwidth yield  $W=1-2$  eV,<sup>15-17</sup> experimental data propose  $W=3-4$  eV.<sup>18,19</sup> The exchange coupling  $J$  is not very well known; the  $J=1$  eV of Refs. 15 and 20 is sometimes questioned as being too small.<sup>21</sup> In any case, the manganites belong to the strongly coupled FKLM which cannot be treated perturbatively with respect to  $J$ . The FKLM will certainly be unable to reproduce all the details of the rich phase diagram of  $\text{La}_{1-x}\text{Ca}_x\text{MnO}_3$ , according to which the ground state is antiferromagnetic for  $x=0$  and 1 and ferromagnetic for  $x \approx 0.2-0.4$ , with paramagnetic regions and phase separations in between.<sup>12</sup> Nevertheless, the FKLM is thought to give a reasonable framework for at least a qualitative understanding of the interesting physics of the manganites.<sup>22,23</sup>

#### E. Heavy fermions

The above subclasses are all characterized by a ferromagnetic exchange interaction  $J>0$ . The original Kondo-lattice model,<sup>24</sup> however, refers to  $J<0$ , favoring an antiparallel alignment of conduction electron spin and localized spin. This situation is obviously realized in the heavy-fermion systems, which are to be found especially among Ce compounds and which have provoked intensive research activities because of their extraordinary physical properties. Doniach<sup>24</sup> was the first to point out that there should be a phase transi-

tion from a magnetic state for small  $|J|$  to a nonmagnetic Kondo state for large  $|J|$  characterized by a screening of the local moments by the conduction electron spins. The magnetic state is due to the RKKY interaction, which as an effect of second order ( $\sim J^2$ ) is independent of the sign of  $J$ . However, the Kondo screening is of course absent for  $J>0$ , i.e., for all the subclasses discussed above. For most of the heavy-fermion systems, the RKKY coupling favors an antiferromagnetic ordering of the local moments. In  $\text{CeCu}_{6-x}\text{Au}_x$  the competitive behavior of the RKKY and Kondo screening tendencies can be observed by varying the concentration  $x$ .<sup>25</sup>  $\text{CeCu}_6$  ( $x=0$ ) is nonmagnetic because of perfect Kondo screening, while for  $x>0.1$  the RKKY component dominates, causing antiferromagnetic ordering up to  $x=1$  ( $\text{CeCu}_5\text{Au}$ ) with increasing Néel temperature  $T_N$  for increasing  $x$ .

$J<0$  does not necessarily lead to antiferromagnetism. The compound  $\text{CeSi}_x$  is ferromagnetic for  $1.6 \leq x \leq 1.85$ ,<sup>26</sup> with a strongly reduced magnetic moment. The Curie temperature of the ferromagnetic Kondo system ( $J<0$ )  $\text{CeNi}_x\text{Pt}_{1-x}$  first increases between  $x=0$  and  $x=0.5$  from 5.8 K ( $x=0$ ) to about 8.6 K ( $x=0.5$ ), and then decreases rapidly, and disappears eventually at  $x=0.55$ .<sup>27</sup> The magnetic moment per Ce ion diminishes steadily with increasing  $x$  because of increasing Kondo screening and disappears completely at  $x=0.95$ .

The above-presented list documents the rich variety of applications for the KLM. Since the many-body problem of the Hamiltonian (1) has not been solved exactly up to now, approximations must be tolerated. Most of the recent theoretical papers aiming at the CMR materials assume classical spins  $S \rightarrow \infty$ ,<sup>28-30</sup> mainly in order to be able to apply dynamical mean field theory (DMFT) to the FKLM problem. The merits of DMFT, e.g., with respect to the Hubbard model, are indisputable, but the assumption of classical spins in the KLM appears very problematic. Several important features, such as, e.g., magnon emission and absorption by the itinerant electrons, are excluded from the very beginning. The importance of such effects has been discussed in detail in Ref. 10. Conclusions such as that at  $T=0$  the spins of the  $e_g$  electrons are oriented parallel to the  $t_{2g}$  spins<sup>30</sup> are correct only for  $S \rightarrow \infty$ . For any finite spin, there is a considerable amount of  $\downarrow$  spectral weight overlapping with  $\uparrow$  states even for very large  $J$ . Recently, a DMFT-based approach to the KLM with quantum spins has been proposed,<sup>31</sup> which uses a fermionization of the local spin operators. The theory is restricted to  $S=1/2$  but retains the quantum nature of the spins. Band splitting, which occurs already for relatively low interaction strengths, can be related to distinct elementary excitations, namely, magnon emission and absorption by the itinerant electron and the formation of magnetic polarons. The results, which are in remarkable agreement with those from the moment conserving decoupling approach (MCDA) in Ref. 10, confirm the importance of the quantum nature of the spins.

For various reasons, the above-mentioned theories<sup>10,31</sup> are best justified for weak and intermediate couplings  $J$ . In this paper, we propose an approximate scheme that mainly aims at the strong coupling regime ( $JS \gg W$ , where  $W$  is the bandwidth) but is nevertheless perturbationally correct up to order

$J^2$ . The idea is to construct a self-energy ansatz that interpolates between exactly known limiting cases and reproduces the correct high-energy expansion of the self-energy. To demonstrate the method as clearly as possible, we restrict our consideration to the low-concentration region, performing a detailed calculation for a single electron in an otherwise empty conduction band. The theory is outlined in Sec. II, while Sec. III is a discussion of the results.

## II. THEORY

### A. The many-body problem

The model Hamiltonian (1) defines a nontrivial many-body problem, the exact solution of which is known only for a small number of special cases. For practical reasons, it is sometimes more convenient to use the second quantized form of the exchange interaction (3):

$$H_{sf} = -\frac{1}{2}J \sum_{j\sigma} (z_\sigma S_j^z n_{j\sigma} + S_j^{-\sigma} c_{j-\sigma}^\dagger c_{j\sigma}). \quad (4)$$

Here we have used the abbreviations

$$n_{j\sigma} = c_{j\sigma}^\dagger c_{j\sigma}, \quad z_\sigma = \delta_{\sigma\uparrow} - \delta_{\sigma\downarrow}, \quad S_j^\sigma = S_j^x + i z_\sigma S_j^y. \quad (5)$$

The first term in Eq. (4) describes an Ising-like interaction between the  $z$  components of the localized and itinerant spins. The second term refers to spin exchange processes between the two subsystems.

If we are mainly interested in the conduction electron properties, then the single-electron Green function

$$G_{ij\sigma}(E) = \langle\langle c_{i\sigma}; c_{j\sigma}^\dagger \rangle\rangle_E \quad (6)$$

is of primary interest. Its equation of motion reads

$$\begin{aligned} & \sum_m (E \delta_{im} - T_{im}) G_{mj\sigma}(E) \\ &= \hbar \delta_{ij} - \frac{1}{2} J [z_\sigma I_{ii,j\sigma}(E) + F_{ii,j\sigma}(E)] \end{aligned} \quad (7)$$

where the two types of interaction term in Eq. (4) lead to the spin-flip function

$$F_{im,j\sigma}(E) = \langle\langle S_i^{-\sigma} c_{m-\sigma}; c_{j\sigma}^\dagger \rangle\rangle_E \quad (8)$$

and the Ising function

$$I_{im,j\sigma}(E) = \langle\langle S_i^z c_{m\sigma}; c_{j\sigma}^\dagger \rangle\rangle_E. \quad (9)$$

The two higher Green functions on the right-hand side of Eq. (7) prevent a direct solution of the equation of motion. A formal solution for the Fourier-transformed single-electron Green function

$$G_{\mathbf{k}\sigma}(E) = \langle\langle c_{\mathbf{k}\sigma}; c_{\mathbf{k}\sigma}^\dagger \rangle\rangle_E = \frac{\hbar}{E - \epsilon(\mathbf{k}) - \Sigma_{\mathbf{k}\sigma}(E)} \quad (10)$$

defines the in general complex self-energy  $\Sigma_{\mathbf{k}\sigma}(E)$  by the ansatz

$$\langle\langle [H_{sf}, c_{\mathbf{k}\sigma}]_-; c_{\mathbf{k}\sigma}^\dagger \rangle\rangle_E = \Sigma_{\mathbf{k}\sigma}(E) G_{\mathbf{k}\sigma}(E). \quad (11)$$

$\epsilon(\mathbf{k})$  are the Bloch energies

$$\epsilon(\mathbf{k}) = \frac{1}{N} \sum_{i,j} T_{ij} e^{i\mathbf{k} \cdot (\mathbf{R}_i - \mathbf{R}_j)}. \quad (12)$$

An illustrative quantity that we are going to discuss in the following is the quasiparticle density of states (Q-DOS):

$$\rho_\sigma(E) = -\frac{1}{\hbar \pi N} \sum_{\mathbf{k}} \text{Im} G_{\mathbf{k}\sigma}(E + i0^+). \quad (13)$$

For the general case neither  $\Sigma_{\mathbf{k}\sigma}(E)$  nor  $G_{\mathbf{k}\sigma}(E)$  can be determined exactly. However, some rigorous statements are possible and will now be listed.

### B. Zero-bandwidth limit

The final goal of our study is to arrive at a self-energy formula that is credible first of all in the strong coupling limit ( $JS \gg W$ ). That means, in particular, that our approach has to satisfy the exactly solvable zero-bandwidth case<sup>32</sup>:

$$T_{ij} \rightarrow T_0 \delta_{ij}, \quad \epsilon(\mathbf{k}) \rightarrow T_0 \forall \mathbf{k}. \quad (14)$$

The conduction band is shrunk to an  $N$ -fold degenerate level  $T_0$ . The localized spin system, however, is further on considered as collectively ordered for  $T < T_c$  by any direct or indirect exchange interaction. The latter is not a part of the KLM. The localized magnetization  $\langle S^z \rangle$  therefore enters the calculation as an external parameter. With Eq. (14), the hierarchy of equations of motion for the single-electron Green function  $G_{ij}(E)$ , following from Eq. (7), decouples exactly.<sup>32</sup> The result is a four-pole function

$$G_{ii\sigma}^{(W=0)}(E) = \sum_{j=1}^4 \frac{\alpha_{j\sigma}}{E - E_{j\sigma}} \quad (15)$$

with spin-independent poles at

$$E_{1\sigma} = T_0 - \frac{1}{2} JS, \quad E_{2\sigma} = T_0 + \frac{1}{2} J(S+1), \quad (16)$$

$$E_{3\sigma} = T_0 - \frac{1}{2} J(S+1), \quad E_{4\sigma} = T_0 + \frac{1}{2} JS. \quad (17)$$

The  $j=1,2$  excitations [Eq. (16)] refer to singly occupied sites; more strictly, they appear when the test electron is brought to a site where no other conduction electron is present. It then orients its spin parallel ( $E_{1\sigma}$ ) or antiparallel ( $E_{2\sigma}$ ) to the local spin. These excitations are bound to spin-dependent spectral weights

$$\alpha_{1\sigma} = \frac{1}{2S+1} \{S+1 + m_\sigma + \Delta_{-\sigma} - (S+1) \langle n_{-\sigma} \rangle\}, \quad (18)$$

$$\alpha_{2\sigma} = \frac{1}{2S+1} \{S - m_\sigma - \Delta_{-\sigma} - S \langle n_{-\sigma} \rangle\}. \quad (19)$$

Here we have abbreviated

$$m_\sigma = z_\sigma \langle S^z \rangle, \quad (20)$$

$$\Delta_\sigma = \langle S_i^\sigma c_{i-\sigma}^\dagger c_{i\sigma} \rangle + z_\sigma \langle S_i^z n_{i\sigma} \rangle. \quad (21)$$

The mixed correlation function  $\Delta_\sigma$  can be derived via the spectral theorem from the Ising and spin-flip functions (8) and (9). Exploiting the equation of motion (7), this can even be expressed in terms of the single-electron Green function:

$$\Delta_\sigma = -\frac{1}{\pi\hbar} \frac{1}{N} \sum_{\mathbf{k}} \int_{-\infty}^{+\infty} dE f_{-}(E) [E - \epsilon(\mathbf{k})] \text{Im} G_{\mathbf{k}\sigma}(E) \quad (22)$$

where  $f_{-}(E) = (1 + e^{\beta(E-\mu)})^{-1}$  is the Fermi function ( $\mu$  is the chemical potential). Similarly, for the spin-dependent particle numbers

$$\langle n_\sigma \rangle = -\frac{1}{\pi\hbar} \frac{1}{N} \sum_{\mathbf{k}} \int_{-\infty}^{+\infty} dE f_{-}(E) \text{Im} G_{\mathbf{k}\sigma}(E). \quad (23)$$

The expectation values in the spectral weights  $\alpha_{1,2\sigma}$  are, therefore, all self-consistently determinable by the required single-electron Green function itself.

The two other poles  $E_{3\sigma}$  and  $E_{4\sigma}$  are bound to double occupancies of the lattice site. The test electron enters a site that is already occupied by another electron with opposite spin. The corresponding spectral weights

$$\alpha_{3\sigma} = \frac{1}{2S+1} \{S \langle n_{-\sigma} \rangle - \Delta_{-\sigma}\}, \quad (24)$$

$$\alpha_{4\sigma} = \frac{1}{2S+1} \{(S+1) \langle n_{-\sigma} \rangle + \Delta_{-\sigma}\}, \quad (25)$$

vanish in the limit of zero band occupation. It may be considered a shortcoming of the KLM that the excitation energies (17) do not contain the Coulomb interaction energy. Switching on a Hubbard interaction  $U$  leads to an additive term  $U$  in  $E_{3\sigma}$  as well as in  $E_{4\sigma}$ ,<sup>32</sup> shifting these excitations to higher energies. While the Hubbard  $U$  is of course the exact ansatz in the zero-bandwidth limit, it is not so obvious by what type of Coulomb interaction the KLM should be extended [the correlated KLM (Ref. 30)] when aiming at one of the subclasses described in the Introduction. To avoid this ambiguity we restrict our following consideration to the low-density limit ( $n \rightarrow 0$ ), where the self-energy of the zero-bandwidth KLM reads according to Eqs. (16)–(19)

$$\Sigma_\sigma^{(W=0)}(E) \rightarrow \frac{n \rightarrow 0 \quad \frac{1}{4} J^2 S(S+1) - \frac{1}{2} J m_\sigma (E - T_0)}{E - T_0 - \frac{1}{2} J (m_\sigma + 1)}. \quad (26)$$

This rigorous result will be exploited later for testing our approximate theory.

### C. Ferromagnetically saturated semiconductor

There is another very instructive limiting case that can be treated exactly. It concerns a single electron in an otherwise empty conduction band interacting with a ferromagnetically saturated local moment system ( $T=0$ ). In the zero-bandwidth limit (Sec. II B) for the  $\uparrow$  spectrum, all the spectral weights (19), (24), and (25) disappear, except for  $\alpha_{1\uparrow} = 1$ . In the  $\downarrow$  spectrum the levels  $E_{1\downarrow}$  and  $E_{2\downarrow}$  survive with the weights  $\alpha_{1\downarrow} = 1/(2S+1)$  and  $\alpha_{2\downarrow} = 2S/(2S+1)$ .

For finite bandwidth, the special case mentioned is that of a ferromagnetically saturated semiconductor (EuO at  $T=0$ ).<sup>10,31,33–35</sup> In this situation, an  $\uparrow$  electron has no chance for a spin flip, the corresponding quasiparticle density of states  $\rho_\uparrow(E)$  is therefore only rigidly shifted compared to the free DOS,<sup>10</sup> and the self-energy is a constant:

$$\Sigma_{\mathbf{k}\uparrow}^{(T=0, n=0)}(E) = \Sigma_{\uparrow}^{(T=0, n=0)}(E) = -\frac{1}{2} JS. \quad (27)$$

The  $\downarrow$  spectrum is more complicated since a  $\downarrow$  electron has several possibilities to exchange its spin with the antiparallel, localized spins. The spin-flip function (8) does not vanish as in the  $\uparrow$  case. Nevertheless, the problem is exactly solvable, resulting in a wave-vector-independent self-energy:

$$\Sigma_{\downarrow}^{(T=0, n=0)}(E) = \frac{1}{2} JS \left( 1 + \frac{JG_0\left(E + \frac{1}{2} JS\right)}{1 - \frac{1}{2} JG_0\left(E + \frac{1}{2} JS\right)} \right). \quad (28)$$

$G_0(E)$  is the free propagator:

$$G_0(E) = \frac{1}{N} \sum_{\mathbf{k}} G_{\mathbf{k}}^{(0)}(E) = \frac{1}{N} \sum_{\mathbf{k}} \frac{1}{E - \epsilon(\mathbf{k})}. \quad (29)$$

The reason for the wave-vector independence of the self-energy can be traced back<sup>10</sup> to the lack of a direct (Heisenberg) exchange term in the model Hamiltonian (1). Therefore  $\Sigma_{\downarrow}^{(T=0, n=0)}(E)$  does not contain magnon energies  $\hbar\omega(\mathbf{q})$  which come into play when the excited  $\downarrow$  electron flips its spin by magnon emission. Neglecting the exchange between the local-moment spins  $\mathbf{S}_i$  may be considered as the  $\hbar\omega(\mathbf{q}) \equiv 0$  case. As a consequence, the electronic self-energy becomes wave-vector independent. No problem arises in calculating the limit ( $n=0, T=0$ ) with the inclusion of a Heisenberg exchange ( $\sim J_{ij} \mathbf{S}_i \cdot \mathbf{S}_j$ ). Then the wave-vector dependence of the self-energy reappears.<sup>10</sup>

### D. Second-order perturbation theory

Conventional diagrammatic perturbation theory for the Kondo-lattice model does not work because of the lack of Wick's theorem. A fertile alternative is the Mori formalism,<sup>36,37</sup> which allows for a systematic expansion of the electronic self-energy of the KLM with respect to the powers of  $J$ . That has successfully been done previously for the weakly coupled Hubbard model by use of the modified perturbation theory of Refs. 38 and 39. In the case of the KLM, the first-order term is just the mean field result  $\frac{1}{2} J m_\sigma$ , while in the second order one finds [Eq. (3.12) in Ref. 39]

$$\Sigma_{\mathbf{k}\sigma}^{(2)}(E) \rightarrow \frac{J^2}{4N^2} \sum_{\mathbf{q}} \left\{ \langle S_{-\mathbf{q}}^\sigma S_{\mathbf{q}}^\sigma \rangle^{(1)} G_{\mathbf{k}+\mathbf{q}}^{(0)} \left( E - \frac{1}{2} J m_\sigma \right) + \langle \delta S_{-\mathbf{q}}^z \cdot \delta S_{\mathbf{q}}^z \rangle^{(1)} G_{\mathbf{k}+\mathbf{q}}^{(0)} \left( E + \frac{1}{2} J m_\sigma \right) \right\}. \quad (30)$$

$\langle \dots \rangle^{(1)}$  means mean field averaging, while the  $\mathbf{q}$ -dependent spin operator is defined as usual,



$$S_{\mathbf{q}}^{\alpha} = \sum_i S_i^{\alpha} e^{-i\mathbf{q}\cdot\mathbf{R}_i} \quad (\alpha = +, -, z). \quad (31)$$

$\delta S_{\mathbf{q}}^z$  is a shorthand notation:

$$\delta S_{\mathbf{q}}^z = S_{\mathbf{q}}^z - \langle S_{\mathbf{q}}^z \rangle^{(1)}. \quad (32)$$

In the following we are interested in the local self-energy  $\Sigma_{\sigma}(E) = (1/N) \sum_{\mathbf{k}} \Sigma_{\mathbf{k}\sigma}(E)$  only, which we find with Eq. (30) up to order  $J^2$  in the limit  $n \rightarrow 0$  to be

$$\begin{aligned} \Sigma_{\sigma}(E) &= -\frac{1}{2} J m_{\sigma} + \frac{1}{4} J^2 \{S(S+1) - m_{\sigma}(m_{\sigma}+1)\} G_0(E) \\ &\quad + O(J^3). \end{aligned} \quad (33)$$

### E. High-energy expansions

For controlling unavoidable approximations, the spectral moments  $M_{\mathbf{k}\sigma}^{(n)}$  of the spectral density  $S_{\mathbf{k}\sigma}(E)$

$$S_{\mathbf{k}\sigma}(E) = -\frac{1}{\pi} \text{Im} G_{\mathbf{k}\sigma}(E) \quad (34)$$

are of great importance:

$$M_{\mathbf{k}\sigma}^{(n)} = \frac{1}{\hbar} \int_{-\infty}^{+\infty} dE E^n S_{\mathbf{k}\sigma}(E). \quad (35)$$

In principle, they can be calculated rigorously via the equivalent expression

$$M_{\mathbf{k}\sigma}^{(n)} = \langle \underbrace{[[\cdots [c_{\mathbf{k}\sigma}, H]_{-}, \cdots, H]_{-}, c_{\mathbf{k}\sigma}^{\dagger}]_{+}}_{n\text{-fold}} \rangle. \quad (36)$$

There is a close connection between the spectral moments and the high-energy behavior of the Green function:

$$\begin{aligned} G_{\mathbf{k}\sigma}(E) &= \int_{-\infty}^{+\infty} dE' \frac{S_{\mathbf{k}\sigma}(E')}{E - E'} \\ &= \frac{1}{E} \sum_{n=0}^{\infty} \int_{-\infty}^{+\infty} dE' \left(\frac{E'}{E}\right)^n S_{\mathbf{k}\sigma}(E') = \hbar \sum_{n=0}^{\infty} \frac{M_{\mathbf{k}\sigma}^{(n)}}{E^{n+1}}. \end{aligned} \quad (37)$$

Because of the Dyson equation

$$E G_{\mathbf{k}\sigma}(E) = \hbar + [\epsilon(\mathbf{k}) + \Sigma_{\mathbf{k}\sigma}(E)] G_{\mathbf{k}\sigma}(E) \quad (38)$$

an analogous expansion holds for the self-energy:

$$\Sigma_{\mathbf{k}\sigma}(E) = \sum_{m=0}^{\infty} \frac{C_{\mathbf{k}\sigma}^{(m)}}{E^m}. \quad (39)$$

The coefficients  $C_{\mathbf{k}\sigma}^{(m)}$  turn out to be simple functions of the moments up to order  $m+1$ :

$$C_{\mathbf{k}\sigma}^{(0)} = M_{\mathbf{k}\sigma}^{(1)} - \epsilon(\mathbf{k}), \quad (40)$$

$$C_{\mathbf{k}\sigma}^{(1)} = M_{\mathbf{k}\sigma}^{(2)} - (M_{\mathbf{k}\sigma}^{(1)})^2, \quad (41)$$

$$C_{\mathbf{k}\sigma}^{(2)} = M_{\mathbf{k}\sigma}^{(3)} - 2M_{\mathbf{k}\sigma}^{(2)}M_{\mathbf{k}\sigma}^{(1)} + (M_{\mathbf{k}\sigma}^{(1)})^3. \quad (42)$$

Using the definition (36), the moments of the KLM can be explicitly calculated by the use of the model Hamiltonian (1). After tedious but straightforward manipulations, one finds in the low-density limit ( $n \rightarrow 0$ ), for the first four moments,

$$M_{\mathbf{k}\sigma}^{(0)} = 1, \quad (43)$$

$$M_{\mathbf{k}\sigma}^{(1)} = \epsilon(\mathbf{k}) - \frac{1}{2} J m_{\sigma}, \quad (44)$$

$$M_{\mathbf{k}\sigma}^{(2)} = \epsilon^2(\mathbf{k}) - J m_{\sigma} \epsilon(\mathbf{k}) + \frac{1}{4} J^2 [S(S+1) - m_{\sigma}], \quad (45)$$

$$\begin{aligned} M_{\mathbf{k}\sigma}^{(3)} &= \epsilon^3(\mathbf{k}) - \frac{3}{2} J m_{\sigma} \epsilon^2(\mathbf{k}) + \frac{1}{4} J^2 \{A_{\sigma}(\mathbf{k}) + B(\mathbf{k}) + 2\epsilon(\mathbf{k}) \\ &\quad \times [S(S+1) - m_{\sigma}]\} + \frac{1}{8} J^3 \{S(S+1)(1 - m_{\sigma}) - m_{\sigma}\}. \end{aligned} \quad (46)$$

$A_{\sigma}(\mathbf{k})$  and  $B(\mathbf{k})$  are related to spin-correlation functions:

$$A_{\sigma}(\mathbf{k}) = \frac{1}{N} \sum_{i,j} e^{i\mathbf{k}\cdot(\mathbf{R}_i - \mathbf{R}_j)} T_{ij} \langle S_i^{-\sigma} S_j^{\sigma} \rangle, \quad (47)$$

$$B(\mathbf{k}) = \frac{1}{N} \sum_{i,j} e^{i\mathbf{k}\cdot(\mathbf{R}_i - \mathbf{R}_j)} T_{ij} \langle S_i^z S_j^z \rangle. \quad (48)$$

Inserting these expressions into Eqs. (40)–(42) we get for the first three self-energy coefficients

$$C_{\mathbf{k}\sigma}^{(0)} = -\frac{1}{2} J m_{\sigma}, \quad (49)$$

$$C_{\mathbf{k}\sigma}^{(1)} = -\frac{1}{4} J^2 [S(S+1) - m_{\sigma}(m_{\sigma}+1)], \quad (50)$$

$$\begin{aligned} C_{\mathbf{k}\sigma}^{(2)} &= -\frac{1}{4} J^2 [A_{\sigma}(\mathbf{k}) + B(\mathbf{k}) - \epsilon(\mathbf{k}) m_{\sigma}^2] \\ &\quad + \frac{1}{8} J^3 (1 + m_{\sigma}) [S(S+1) - m_{\sigma}(m_{\sigma}+1)]. \end{aligned} \quad (51)$$

They determine the high-energy behavior of the self-energy (39).

### F. Interpolation formula

We want to construct an approximate expression for the electronic self-energy of the low-density KLM, which fulfills the zero-bandwidth limit (26) for all temperatures  $T$  and arbitrary coupling strengths  $J$ , as well as the exact  $T=0$  result (27) and (28) for arbitrary bandwidths and couplings. Furthermore, it should reproduce the correct high-energy (strong coupling) behavior (39) and in addition also the weak coupling result (33). Guided by the nontrivial ( $n=0, T=0$ ) result (28), we start with the following ansatz for the local self-energy:

$$\Sigma_{\sigma}(E) = -\frac{1}{2}Jm_{\sigma} + \frac{1}{4}J^2 \frac{a_{\sigma}G_0\left(E - \frac{1}{2}Jm_{\sigma}\right)}{1 - b_{\sigma}G_0\left(E - \frac{1}{2}Jm_{\sigma}\right)}. \quad (52)$$

$a_{\sigma}$  and  $b_{\sigma}$  are at first unknown parameters. It is easy to recognize that this ansatz reproduces the exact limit (27) and (28) of ferromagnetic saturation, if  $T=0, n=0$ ,

$$a_{\sigma} = (1 - z_{\sigma})S, \quad b_{\downarrow} = \frac{1}{2}J, \quad b_{\uparrow} \text{ arbitrary}, \quad (53)$$

and the zero-bandwidth limit (26), if

$$\epsilon(\mathbf{k}) \rightarrow T_0 \forall \mathbf{k},$$

$$a_{\sigma} = S(S+1) - m_{\sigma}(m_{\sigma}+1), \quad (54)$$

$$b_{\sigma} = b_{-\sigma} = \frac{1}{2}J.$$

We note that Eq. (54) agrees with Eq. (53) for  $T=0$ .

By Eq. (52), we concentrate from the very beginning on the local part of the self-energy. As already stated above, the wave-vector dependence of the self-energy is mainly due to magnon energies  $\hbar\omega(\mathbf{q})$  appearing at finite temperature in magnon emission and absorption processes by the band electron. However, the neglect of a direct Heisenberg exchange between the localized spins in the KLM can be interpreted as the  $\hbar\omega(\mathbf{q}) \rightarrow 0$  limit.

We fix the parameters  $a_{\sigma}$  and  $b_{\sigma}$  in the ansatz (52) by equating it to the high-energy expansion (39). For this purpose, we first develop Eq. (52) in terms of powers of the inverse energy. That requires the respective high-energy expression of the mean field propagator  $G_0(E - \frac{1}{2}Jm_{\sigma})$ , which is exactly known:

$$G_0\left(E - \frac{1}{2}Jm_{\sigma}\right) = \sum_{n=0}^{\infty} \frac{\hat{M}_{\sigma}^{(n)}}{E^{n+1}}, \quad (55)$$

$$\hat{M}_{\sigma}^{(n)} = \frac{1}{N} \sum_{\mathbf{k}} \left( \epsilon(\mathbf{k}) + \frac{1}{2}Jm_{\sigma} \right)^n. \quad (56)$$

From Eq. (52) it then follows that

$$\begin{aligned} \Sigma_{\sigma}(E) &= -\frac{Jm_{\sigma}}{2} + \frac{J^2 a_{\sigma}}{4} \sum_{m=0}^{\infty} \frac{\hat{M}_{\sigma}^{(m)}}{E^{m+1}} \sum_{p=0}^{\infty} \left[ b_{\sigma} \sum_{n=0}^{\infty} \frac{\hat{M}_{\sigma}^{(n)}}{E^{n+1}} \right]^p \\ &= -\frac{1}{2}Jm_{\sigma} + \frac{1}{E} \left\{ \frac{1}{4}J^2 \hat{M}_{\sigma}^{(0)} a_{\sigma} \right\} \\ &\quad + \frac{1}{E^2} \left\{ \frac{1}{4}J^2 a_{\sigma} [\hat{M}_{\sigma}^{(1)} + b_{\sigma} (\hat{M}_{\sigma}^{(0)})^2] \right\} + O(1/E^3). \end{aligned} \quad (57)$$

The local self-energy coefficients thus derived,

$$C_{\sigma}^{(m)} = \frac{1}{N} \sum_{\mathbf{k}} C_{\mathbf{k}\sigma}^{(m)}, \quad (58)$$

$$C_{\sigma}^{(0)} = -\frac{1}{2}Jm_{\sigma}, \quad (59)$$

$$C_{\sigma}^{(1)} = \frac{1}{4}J^2 a_{\sigma}, \quad (60)$$

$$C_{\sigma}^{(2)} = \frac{1}{4}J^2 a_{\sigma} \left( T_0 + \frac{1}{2}Jm_{\sigma} + b_{\sigma} \right), \quad (61)$$

can be compared to the exact expressions following from Eqs. (49)–(51):

$$C_{\sigma}^{(0)} = -\frac{1}{2}Jm_{\sigma}, \quad (62)$$

$$C_{\sigma}^{(1)} = \frac{1}{4}J^2 [S(S+1) - m_{\sigma}(m_{\sigma}+1)], \quad (63)$$

$$C_{\sigma}^{(2)} = \frac{1}{4}J^2 \left( T_0 + \frac{1}{2}J(1+m_{\sigma}) \right) [S(S+1) - m_{\sigma}(m_{\sigma}+1)]. \quad (64)$$

$C_{\sigma}^{(0)}$  is identically fulfilled. Agreement for the two other coefficients is achieved by setting

$$a_{\sigma} = S(S+1) - m_{\sigma}(m_{\sigma}+1), \quad (65)$$

$$b_{\sigma} = \frac{1}{2}J = b_{-\sigma}. \quad (66)$$

These are the same expressions as found in Eq. (54) for the special zero-bandwidth limit.

Inserting Eqs. (65) and (66) into Eq. (52) yields a self-energy result that is exact for  $T=0$  ( $m_{\sigma} = z_{\sigma}S$ ) but arbitrary bandwidths  $W$  and exchange couplings  $J$ . It fulfills the zero-bandwidth limit for all couplings  $J$  and all temperatures  $T$ . It obeys the high-energy behavior which is important for the strong coupling regime. Furthermore, comparison with Eq. (33) shows that the approach fits second-order perturbation theory, thus being reliable in the weak coupling regime also. We believe that Eq. (52) together with Eqs. (65) and (66) represents a trustworthy approach to the low-density self-energy of the Kondo-lattice model. In the next section we present a numerical evaluation.

### III. RESULTS

We have evaluated our theory for a sc lattice using the respective Bloch density of states (B-DOS) in the tight-binding approximation.<sup>40</sup> The center of gravity  $T_0$  of the Bloch band is chosen as energy zero. Figure 1 shows the temperature-dependent quasiparticle density of states  $\rho_{\sigma}(E)$  for a strongly coupled system ( $J=2.0$  eV,  $S=7/2$ ,  $W=1$  eV). The electronic spectrum gets its temperature dependence exclusively through the local-moment magnetization  $m = |m_{\sigma}| = |\langle S^z \rangle|$ , which must be considered as an external parameter.  $m=3.5$  means  $T=0$  K (ferromagnetic saturation), while  $m=0$  occurs at  $T=T_c$ . The Q-DOS for each spin direction consists of two subbands separated by an energy of the order of  $\frac{1}{2}J(2S+1)$ . They originate from the two atomic levels  $E_{1\sigma}$  and  $E_{2\sigma}$  in the zero-bandwidth limit (16).

A special case is ferromagnetic saturation, for which the  $\uparrow$  spectrum consists only of the undeformed low-energy band [ $\rho_{\uparrow}(E) = \rho_0(E + \frac{1}{2}JS)$ ]. The  $\uparrow$  electron has no chance to exchange its spin with the perfectly aligned local-spin system. The spin-flip terms in the exchange interaction (4) therefore do not work; only the Ising-like part [first term in Eq. (4)] is important for a rigid shift of the excitation spectrum. The  $\downarrow$  spectrum is more complicated because a  $\downarrow$  electron can, even

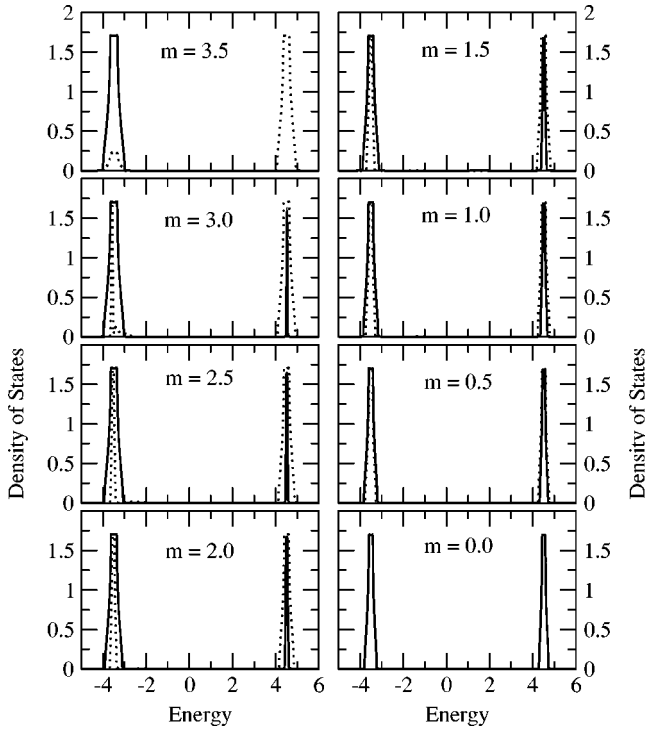


FIG. 1. Quasiparticle density of states as a function of energy for various values of magnetization. Full line for spin up and dotted line for spin down.  $J=2$ ,  $S=7/2$ , and  $W=1$ .

at  $T=0$  K, exchange its spin with the ferromagnetically saturated spin system. One possibility is to emit a magnon, thereby reversing its own spin and becoming a  $\uparrow$  electron. Such a spin-flip excitation is, of course, possible only if there are  $\uparrow$  states within reach on which the original  $\downarrow$  electron can land after the spin flip. That is the reason why the low-energy  $\downarrow$  subband occupies the same energy region as the  $\uparrow$  band.

The  $\downarrow$  electron has another possibility to exchange its spin with the ferromagnetically saturated moment system by repeated magnon emission and reabsorption. In a certain sense the electron propagates through the lattice dressed by a virtual cloud of magnons. For the parameters chosen in Fig. 1, this gives rise even to the formation of a stable quasiparticle, which we call the magnetic polaron.<sup>10,35</sup> The polaron states form, at  $T=0$  K, the upper  $\downarrow$  quasiparticle subband. It goes without saying that polaron formation is impossible for the  $\uparrow$  electron in a saturated moment system. Therefore no upper quasiparticle subband appears in the  $\uparrow$  spectrum. This changes for finite temperatures.

For  $T>0$  ( $m<3.5$ ) the  $\uparrow$  spectrum too becomes more structured because the localized spin system is no longer perfectly aligned. The system now contains magnons that can be absorbed by the  $\uparrow$  electron. Even polaron formation becomes possible. The spectral weight of the upper  $\uparrow$  quasiparticle subband rises with increasing temperature, i.e., increasing magnon density. Figure 1 illustrates that the temperature dependence of the Q-DOS mainly affects the spectral weights of the subbands and not so much their positions. This is a typical feature of the strong coupling regime  $JS \gg W$ . In such a situation, the band electron mobility is rather poor; it stays for a relatively long time at the same

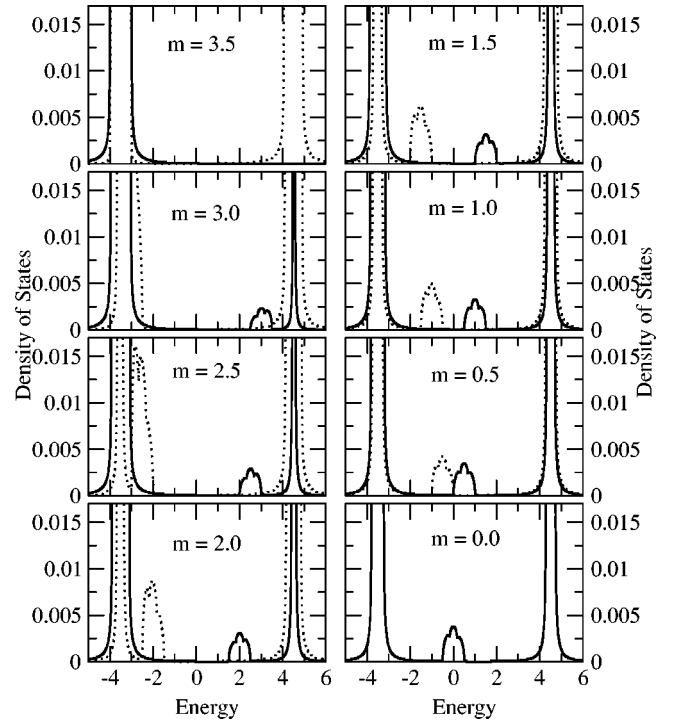


FIG. 2. Same as in Fig. 1 but with enlarged vertical scale.

lattice site. The actual quantization axis is then the localized spin ( $S=7/2$ ), to which the electron can orient its spin parallel (“spin up” in the local frame) or antiparallel (“spin down” in the local frame). The excitation energy for a parallel alignment roughly amounts to  $-\frac{1}{2}JS$ , and for an antiferromagnetic alignment to  $+\frac{1}{2}J(S+1)$ . The lower quasiparticle subband consists of states belonging to the situation where the band electron appears in the local frame as a spin up electron. This may happen directly or after emitting/absorbing a magnon. In the upper subband the electron has entered the local frame as a spin down electron. This is impossible for a  $\uparrow$  electron at  $T=0$  K, when all localized spins are parallel aligned ( $m=S$ ). While the excitation energies are almost temperature independent, the probability for the electron to be in the local frame as a spin up or as a spin down particle strongly depends on temperature. That manifests itself in the spectral weight of the respective quasiparticle subband, which therefore is temperature and spin dependent. There remains a small probability that the band electron is not trapped by the localized spin, but rather propagates with high mobility through the spin lattice. In such a case the effective quantization axis is no longer the local spin but rather the direction of the global magnetization  $\langle S^z \rangle$ . Figure 2 shows the Q-DOS for the same parameters as in Fig. 1 but on a finer scale. One recognizes two tiny satellites which emerge from the two main peaks with increasing temperature (decreasing magnetization  $m$ ). The  $\downarrow$  satellite has a lower energy than the  $\uparrow$  satellite. This can be understood as follows. The original  $\downarrow$  electron will predominantly enter the low-energy part of the spectrum by emitting a magnon, thereby reversing its own spin. In case of being not trapped by a local spin, it then moves as a  $\uparrow$  electron through the spin lattice. On the other hand, an original  $\uparrow$  electron has

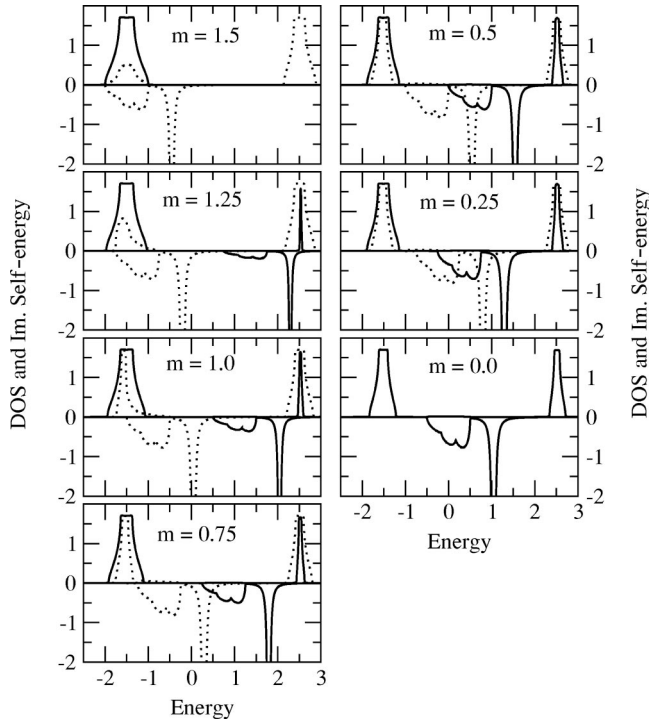


FIG. 3. Quasiparticle density of states (in the positive half of the frame) and imaginary part of the self-energy (in the negative half of the frame) as functions of energy for various values of magnetization. Full line for spin up and dotted line for spin down.  $J=2$ ,  $S=3/2$ , and  $W=1$ .

to absorb a magnon in order to enter the high-energy part of the spectrum and propagate then as a  $\downarrow$  electron. With decreasing magnetization the two satellites collapse mean-field-like. In the strong coupling regime ( $JS \gg W$ ) pictured in Figs. 1 and 2 the satellites have only very small spectral weights, nevertheless representing interesting physics.

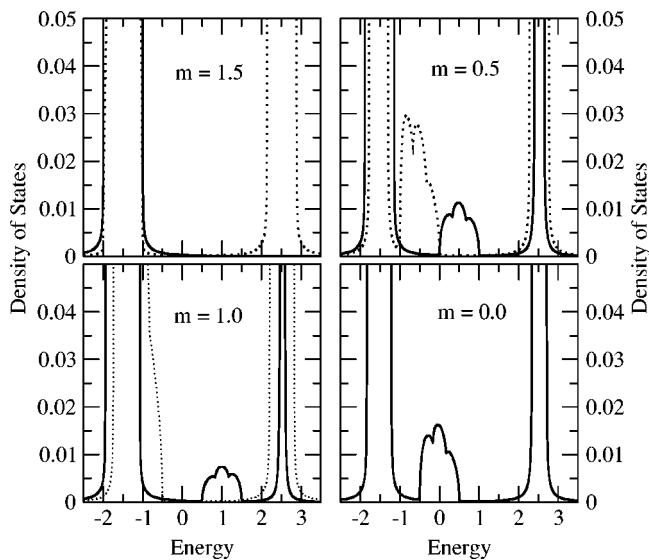


FIG. 4. Quasiparticle density of states as a function of energy for various values of magnetization. Full line for spin up and dotted line for spin down.  $J=2$ ,  $S=3/2$ , and  $W=1$ .

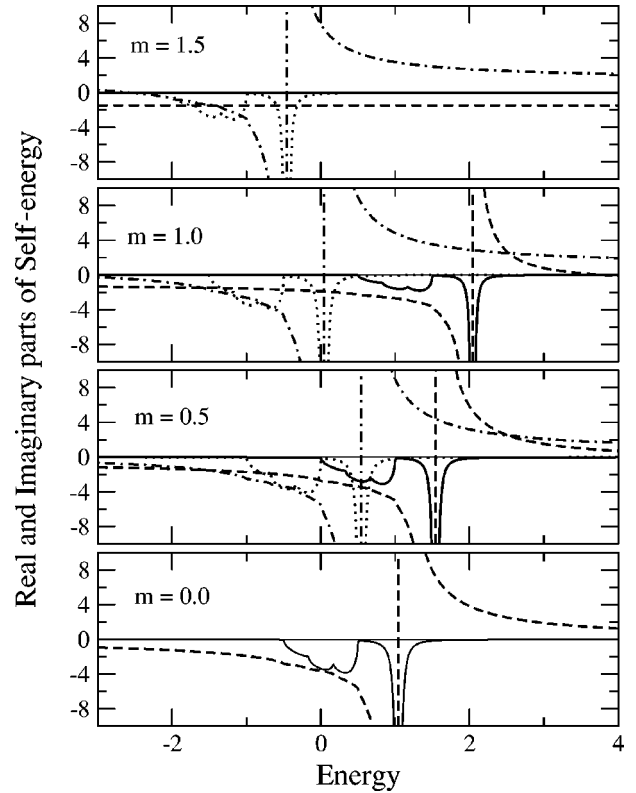


FIG. 5. Real and imaginary parts of the self-energy as a function of energy for different values of magnetization. For imaginary part, full line for spin up and dotted line for spin down. For real part, dashed line for spin up and dash-dotted line for spin down. Imaginary part of the self-energy is multiplied by a factor of 5 for better clarity.  $J=2$ ,  $S=3/2$ , and  $W=1$ .

The parameters used in Figs. 3, 4, and 5 ( $J=2$  eV,  $W=1$ ,  $S=3/2$ ) should be typical for the manganites. It is sometimes claimed<sup>21,30</sup> that because of the strong coupling  $JS$  the itinerant electron ( $e_g$ ) spin is oriented at  $T=0$  K in any case parallel to the localized ( $t_{2g}$ ) spin. According to the exact  $m=S=3/2$  part of Fig. 3, this can be strictly ruled out for the FKLM. In the papers mentioned the assumption of full polarization is an artifact due to the restriction to classical spins ( $S \rightarrow \infty$ ). The temperature dependence of the Q-DOS is of course very similar to the  $S=7/2$  case in Fig. 1. Even the satellites that describe the free electron propagation after emitting/absorbing a magnon appear (Fig. 4). However, because of the smaller distance between the two main peaks [ $\approx \frac{1}{2}J(2S+1)$ ] the mean field shift of the satellites is not so clearly visible as for the higher spin in Fig. 1.

The imaginary part of the self-energy is directly related to quasiparticle damping and lifetime, respectively. Figure 3 demonstrates that the polaron states (upper part of the spectrum) represent quasiparticles with almost infinite lifetimes since  $\text{Im} \Sigma_{\sigma}(E)$  is zero in this region. For  $T=0$  K, this is an exact result. At ferromagnetic saturation the whole  $\uparrow$  spectrum consists of stable states. It turns out that in the strong coupling regime discussed here, even for finite temperatures, only the states of the mean field satellites have finite life-



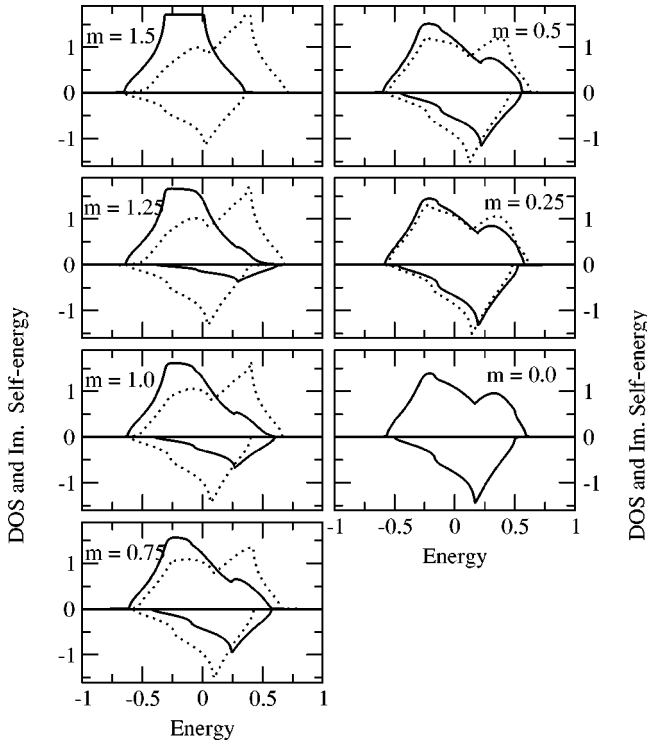


FIG. 6. Quasiparticle density of states (in the positive half of the frame) and imaginary part of the self-energy (in the negative half of the frame) as a function of energy for different values of magnetization. Full line for spin up and dotted line for spin down. Imaginary self-energy is multiplied by a factor of 5 for better clarity.  $J = 0.2$ ,  $S = 3/2$ , and  $W = 1$ .

times. The sharp peak of  $\text{Im} \Sigma_{\sigma}(E)$  always falls in the band gap, which is provoked by a divergence of the real part of the self-energy (Fig. 5). It has therefore no direct influence on the lifetime of the quasiparticles.

Up to now we have only discussed the FKLM in the strong coupling regime. As demonstrated in Sec. IID, our interpolating approach is correct in the weak coupling region too. Figure 6 shows, as an example, the Q-DOS for  $J = 0.2$  eV,  $W = 1$  eV, and  $S = 3/2$ . The tendency to the two-subband structure can be recognized for weak couplings also. The physical interpretation of the responsible elementary processes is the same as in the strong coupling case discussed above. For  $T = 0$  all  $\uparrow$  states represent stable quasiparticles, and the corresponding imaginary part of the self-energy vanishes. With increasing demagnetization of the local moment system,  $\text{Im} \Sigma_{\uparrow}(E)$  becomes finite indicating finite lifetimes of  $\uparrow$  quasiparticles due to magnon absorption, which is impossible at  $T = 0$  because of ferromagnetic saturation. Magnon emission by  $\downarrow$  electrons, however, is always possible. It should be pointed out that the upper part of the  $\downarrow$  spectrum obviously consists, at low temperature, of stable polaron states.

It is surprising that very small couplings are already sufficient to create a pseudogap in the quasiparticle spectrum. According to Fig. 7, which shows the exact  $T = 0 - \rho_{\sigma}(E)$  for various exchange couplings  $J$ , the gap is opened already

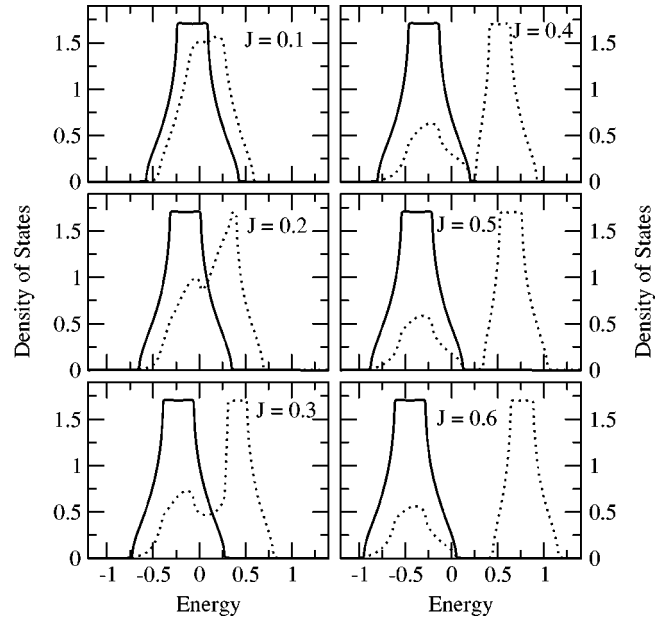


FIG. 7. Quasiparticle density of states as a function of energy for different values of coupling constant  $J$ . Full line for spin up and dotted line for spin down.  $m = 1.5$  (ferromagnetic saturation),  $S = 3/2$ , and  $W = 1$ .

for  $J = 0.4$  eV. Our results for the weakly coupled FKLM are very similar to those presented in Ref. 10.

#### IV. CONCLUSIONS

We have presented an approach to the ferromagnetic Kondo-lattice model in the low-density limit ( $n \rightarrow 0$ ). The theory uses an interpolation formula for the electronic self-energy which fulfills a maximum number of limiting cases. It reproduces the nontrivial rigorous special case of a single electron in an otherwise empty conduction band at  $T = 0$  (ferromagnetically saturated semiconductor), and that for arbitrary bandwidths and coupling constants. It is exact in the zero-bandwidth limit for all temperatures and all exchange couplings. It obeys the high-energy expansion of the self-energy, guaranteeing therewith the right strong coupling behavior, as well as perturbation theory of second order ( $\propto J^2$ ) for the weak-coupling side. All exact criteria available for the ferromagnetic Kondo-lattice model known to us are correctly reproduced by the present low-density approach.

Strong correlation effects due to interband exchange appear in the quasiparticle density of states. A rather weak coupling  $J/W$  already provokes a distinct temperature dependence in the electronic structure, mainly due to spin exchange processes between the localized magnetic moments and itinerant band electrons. Magnon emission/absorption processes compete with polaronlike quasiparticle formation. These facts demonstrate that the assumption of classical spins ( $S \rightarrow \infty$ ), very often used for the simplified treatment of the model,<sup>30</sup> suppresses just the essentials of the Kondo-lattice model. A necessary extension of the theory

presented has to include finite band occupations, which certainly requires additional approximations. The  $n \rightarrow 0$  approach developed here can then serve as a weighty criterion for the correctness of the approach.

## ACKNOWLEDGMENTS

This work was prepared as an India-Germany Partnership Project sponsored by the Volkswagen Foundation.

- 
- <sup>1</sup>W. Nolting, *Phys. Status Solidi B* **96**, 11 (1979).  
<sup>2</sup>P. Wachter, in *Handbook on the Physics and Chemistry of Rare Earths*, edited by K. A. Gschneidner and L. Eyring (Elsevier, Amsterdam, 1979), Vol. 2, p. 507.  
<sup>3</sup>G. Busch, P. Junod, and P. Wachter, *Phys. Rev. Lett.* **12**, 11 (1964).  
<sup>4</sup>J. Kossut, *Phys. Status Solidi B* **78**, 537 (1976).  
<sup>5</sup>L. W. Roeland, G. J. Cock, F. A. Muller, C. A. Mollman, K. A. M. Mc Ewen, R. C. Jordan, D. W. Jones, *J. Phys. F: Met. Phys.* **5**, L233 (1975).  
<sup>6</sup>S. Rex, V. Eyert, W. Nolting, *J. Magn. Magn. Mater.* **192**, 529 (1999).  
<sup>7</sup>*Magnetism and Electronic Correlations in Local Moment Systems: Rare Earth Elements and Compounds*, edited by M. Donath, P. Dowben, and W. Nolting (World Scientific, Singapore, 1998).  
<sup>8</sup>D. Li, J. Zhang, P. A. Dowben, and M. Onellion, *Phys. Rev. B* **45**, 7272 (1992).  
<sup>9</sup>B. Kim, A. B. Andrews, J. L. Erskine, K. J. Kim, and B. N. Harmon, *Phys. Rev. Lett.* **68**, 1931 (1992).  
<sup>10</sup>W. Nolting, S. Rex, and S. Mathi Jaya, *J. Phys.: Condens. Matter* **9**, 1301 (1997).  
<sup>11</sup>S. Jin, T. H. Tiefel, M. Mc Cormack, R. A. Fastnacht, R. Ramesh, and L. H. Chen, *Science* **264**, 413 (1994).  
<sup>12</sup>A. P. Ramirez, *J. Phys.: Condens. Matter* **9**, 8171 (1997).  
<sup>13</sup>W. Nolting, *Quantentheorie des Magnetismus II* (Teubner-Verlag, Stuttgart, 1986), Chap. 5.3.3.  
<sup>14</sup>C. Zener, *Phys. Rev.* **81**, 440 (1951).  
<sup>15</sup>S. Satpathy, Z. S. Popovic, and F. R. Vukajlovic, *Phys. Rev. Lett.* **76**, 960 (1996).  
<sup>16</sup>W. E. Pickett and D. J. Singh, *Phys. Rev. B* **53**, 1146 (1996).  
<sup>17</sup>D. J. Singh and W. E. Pickett, *Phys. Rev. B* **57**, 88 (1998).  
<sup>18</sup>J. H. Park, C. T. Chen, S. W. Cheong, W. Bao, G. Meigs, V. Chakarian, and Y. U. Idzerda, *Phys. Rev. Lett.* **76**, 4215 (1996).  
<sup>19</sup>T. Saitoh, A. Sekiyama, K. Kobayashi, T. Mizokowa, A. Fujimori, D. D. Sarma, Y. Takeda, and M. Takano, *Phys. Rev. B* **56**, 8836 (1997).  
<sup>20</sup>Y. Okimoto, T. Katsufuji, T. Ishikawa, A. Urushibara, T. Arima, and Y. Tokura, *Phys. Rev. Lett.* **75**, 109 (1995).  
<sup>21</sup>A. J. Millis, R. Müller, and B. I. Shraiman, *Phys. Rev. B* **54**, 5405 (1996).  
<sup>22</sup>E. Dagotto, S. Yunoki, A. L. Molvezzi, A. Moreo, J. Hu, S. Capponi, D. Poilblanc, and N. Furukawa, *Phys. Rev. B* **58**, 6414 (1998).  
<sup>23</sup>N. Furukawa, *J. Phys. Soc. Jpn.* **63**, 3214 (1994).  
<sup>24</sup>S. Doniach *Physica B & C* **91B**, 231 (1977).  
<sup>25</sup>H. von Löhneysen, in *Magnetism and Electronic Correlations in Local Moment Systems: Rare Earth Elements and Compounds* (Ref. 7).  
<sup>26</sup>P. Hill, F. Willis, and N. Ali, *J. Phys.: Condens. Matter* **4**, 5015 (1992).  
<sup>27</sup>D. Gignoux and J. C. Gomez-Sal, *Phys. Rev. B* **30**, 3967 (1984).  
<sup>28</sup>N. Furukawa, in *Physics of Manganites*, edited by T. A. Kaplan and S. D. Mahanti (Plenum, New York, 1999), p. 1.  
<sup>29</sup>A. J. Millis, P. B. Littlewood, and B. I. Shraiman, *Phys. Rev. Lett.* **74**, 5144 (1995).  
<sup>30</sup>K. Held and D. Vollhardt, *Phys. Rev. Lett.* **84**, 5168 (2000).  
<sup>31</sup>D. Meyer, C. Santos, and W. Nolting, *J. Phys. Condens Matter* **13**, 2531 (2001).  
<sup>32</sup>W. Nolting and M. Matlak, *Phys. Status Solidi B* **123**, 155 (1984).  
<sup>33</sup>B. S. Shastry and D. C. Mattis, *Phys. Rev. B* **24**, 5340 (1981).  
<sup>34</sup>S. R. Allan and D. M. Edwards, *J. Phys. C* **15**, 2151 (1982).  
<sup>35</sup>W. Nolting, U. Dubil, and M. Matlak, *J. Phys. C* **18**, 3687 (1985).  
<sup>36</sup>H. Mori, *Prog. Theor. Phys.* **33**, 432 (1965).  
<sup>37</sup>H. Mori, *Prog. Theor. Phys.* **34**, 399 (1966).  
<sup>38</sup>G. Bulk and R. J. Jelitto, *Phys. Lett. A* **133**, 231 (1988).  
<sup>39</sup>G. Bulk and R. J. Jelitto, *Phys. Rev. B* **41**, 413 (1990).  
<sup>40</sup>R. J. Jelitto, *J. Phys. Chem. Solids* **30**, 609 (1969).